Ultra-Compact Broadband Dielectric Antenna

Julián L. Pita[1], Paulo Dainese[2], Hugo E. Hernandez-Figueroa[1], and Lucas H. Gabrielli[1,*]

[1] *School of Electrical and Computer Engineering*
[2] *"Gleb Wataghin" Physics Institute*
University of Campinas, 13083-970 Campinas, SP, Brazil

[*] *lucashg@fee.unicamp.br*

Abstract: We demonstrate an ultra-compact silicon on insulator antenna with $3.2\,\mu m^2$ footprint and broadside radiation from 1470 nm to 1550 nm for applications in fiber-to-chip coupling and phased arrays.

OCIS codes: 130.3120, 200.2605.

1. Introduction

In recent years, optical nanoantennas have been employed in a wide variety of applications [1], including sensors [2], microscopy [3], and optical communications [4]. In particular, all-dielectric antennas have been proposed (for example grating-based) in order to overcome large dissipation losses and low radiation efficiency encountered in metallic-based antennas design [5]. However, dielectric antennas still present a relatively large footprint ($8.4\,\mu m^2$) and significant variation with wavelength in the main lobe radiation direction. In this work, we present the design and characterization of an all-dielectric SOI antenna with ultra-compact footprint and wavelength-independent broadside radiation pattern as an alternative to compact gratings.

2. Device design

The nanoantenna design was performed on a silicon region of $3.2\,\mu m^2$ which was subdivided in 4 vertical layers with heights of 0 (fully etched), 70 , 150 or 220 nm (not etched). Only silicon and silicon-oxide materials were considered. The full-vector 3-d electromagnetic simulations were performed using the finite-element method based commercial package COMSOL, and the non-linear optimization was performed with the SNOPT algorithm. The antenna's optimized topology is shown in Fig. 1a, where gray and white colors indicate silicon and silicon oxide regions, respectively. This design was then simplified to comply with fabrication parameters and the resulting structure is shown in Fig. 1b. The device was fabricated at the imec/ePIXfab foundry on an SOI platform with 2 µm of buried silicon dioxide. In Fig. 1c an electron microscope image of the fabricated device is displayed. The full device has a footprint 68% smaller than the reference grating antenna from [5]. The thin output waveguide–top right corner in Fig. 1c–serves to decrease reflections in the device and could also be used for power monitoring.

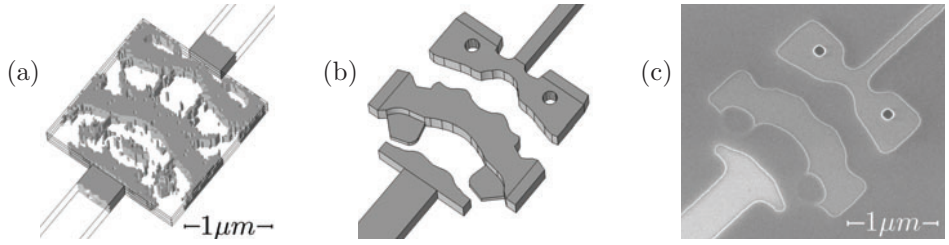

Fig. 1. (a) Optimized antenna design indicating silicon (gray) and silica (white) regions; (b) Simplified design to comply with fabrication process; (c) SEM image of the fabricated prototype.

978-1-943580-11-8/16/$31.00 ©2016 Optical Society of America

3. Results

The near field was measured using the setup shown in Fig. 2a which is composed of a near infrared 20× objective with a 0.4 NA, an imaging lens, and an InGaAs camera. The antenna's input waveguide was excited with a tunable laser source (TLS) coupled via a lensed fiber and an inverse taper at the chip edge. Both grating and our optimized antenna were tested, and the measured near-field patterns are shown in Fig. 2b. For the grating antenna, the near-field pattern presents a significant second-order spot. Moreover, the center position of the main lobe shifts as the input wavelength changes from 1470 nm to 1550 nm. In sharp contrast, the optimized device exhibits no significant second lobe and preserves its broadside radiation pattern almost independent of the excitation wavelength. These results are in agreement with the theoretical modeling. The calculated radiation pattern for each antenna is shown in Fig. 1c. Clearly, the grating's main lobe shifts its direction by approximately 6.5° when the wavelength varies from 1470 nm to 1550 nm. The second-order lobe in the grating antenna pattern is also apparent. Conversely, the far field diagrams of the optimized nanoantenna show that a constant broadside radiation is maintained for the investigated wavelength window.

In summary, we have designed, fabricated and characterized an ultra-compact, broadside radiation, broadband, and all-dielectric nanoantenna. Using a nonlinear numerical optimization process, the final design offers small footprint and a radiation pattern, which keeps its broadside shape for wavelengths ranging from 1470 nm to 1550 nm. These features make it a potential candidate for applications in free-space communications, out-of-plane fiber-to-chip coupling, and optical phased arrays.

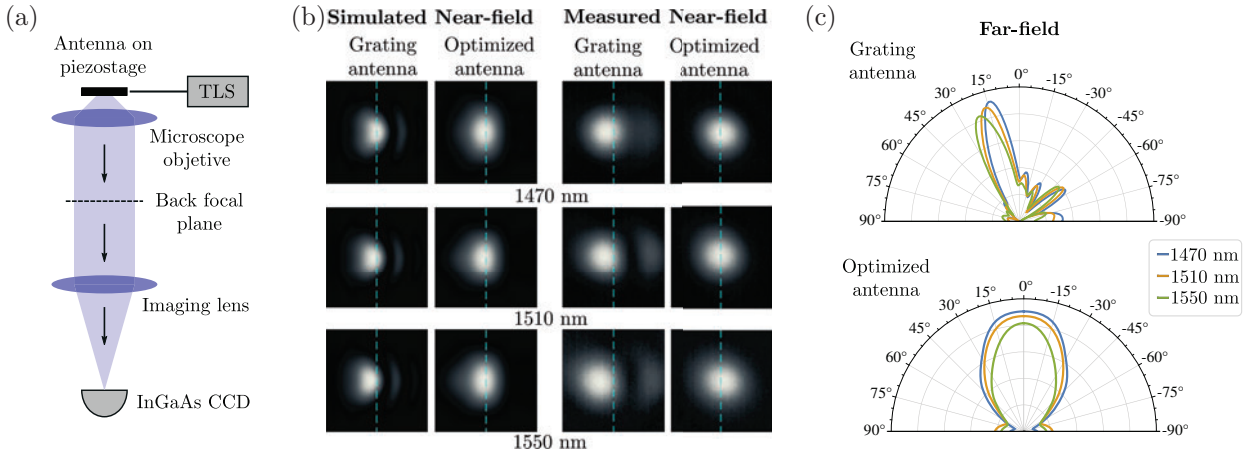

Fig. 2. (a) Experimental setup. (b) Simulated and measured near-field pattern for both grating and optimized antenna for different input wavelengths. (c) Simulated far-field patterns.

Acknowledgements: this work was supported by São Paulo Research Foundation (FAPESP) grants 2013/20180-3, 08/57857-2 and 2012/22517-2, and the National Council for Scientific and Technological Development (CNPq) grants 574017/2008-9 and 446746/2014-2. Julián L. Pita thanks the Coordination for the Improvement of Higher Education Personal (CAPES) for financial support.

References

1. G. N. Malheiros-Silveira, L. H. Gabrielli, C. J. Chang-Hasnain, and H. E. Hernandez-Figueroa, "Breakthroughs in Photonics 2013: Advances in Nanoantennas," IEEE Photonics Journal, vol. 6, no. 2, 7 pages (2014).
2. M. F. Garcia-Parajo, "Optical antennas focus in on biology," Nature Photonics, vol. 2, no. 4, pp. 201–203 (2008).
3. P. Bharadwaj, B. Deutsch, and L. Novotny, "Optical antennas," Advances in Optics and Photonics, vol. 1, no. 3, pp. 438–483 (2009).
4. A. Alù and N. Engheta, "Wireless at the nanoscale: optical interconnects using matched nanoantennas," Physical review letters, vol. 104, no. 21, p. 213902 (2010).
5. J. Sun, E. Timurdogan, A. Yaacobi, E. S. Hosseini, and M. R. Watts, "Large-scale nanophotonic phased array," Nature, vol. 493, no. 7431, pp. 195–199 (2013).